# The Influence of Crystal Material on Intercrystal Scattering and the Parallax Effect in PET Block Detectors: A Monte Carlo Study

S. Lashkari[1,2], S. Sarkar[1,2], M.R. Ay[1,2] and A. Rahmim[3]

[1] Department of Medical Physics and Biomedical Engineering, School of Medicine, Medical Sciences/ Tehran University , Tehran, Iran
[2] Research Center for Science and Technology in Medicine, Medical Sciences/ Tehran University, Tehran, Iran
[3] Department of Radiology, School of Medicine, Johns Hopkins University, Baltimore, USA

*Abstract* — **It is well known that Intercrystal scattering (ICS) and the parallax effect are two major resolution limiting parameters in current PET detector designs with block detectors. More recently for the purpose of resolution recovery, investigators and manufacturers have attempted to accurately model these effects into the image reconstruction task. In this study we utilized the MCNP4C Monte Carlo code to accurately simulate and measure ICS and parallax effects in different crystal materials including BGO, LSO, LYSO, LuAP and GSO. The size of the detector module was fixed at a 52mm × 52 mm crystal array. The results showed that by increasing the incidence angle, the percentage of parallax events was considerably increased, while small increases in the ICS fraction were also observed. The point spread function of the various crystal blocks were also investigated, with BGO crystal showing slightly better FWHM values as well as position detection accuracy. The results indicate that the MCNP4C MC code is a useful tool for investigation of photons interaction in PET block detectors in order to accurately model the ICS and parallax behaviors for the purpose of resolution recovery in the new PET image reconstruction algorithms.**

*Keywords* — **Intercrystal scattering, Resolution recovery, MCNP4C Monte Carlo code, Parallax.**

## I. Introduction

In recent years, PET scanner manufacturers have tried to increase the spatial resolution and detection accuracy of PET scanners by decreasing the crystal size in the block geometry. At the same time, the use of block detectors limits the detection accuracy and decreases the rejection possibility of scattered photons. Additionally, using Anger Logic to determine the position of photons results in mispositioning of the events that originate from multiple compton scattered photons inside the block. This problem leads to blurring of the image. It is well known that intercrystal scattering (ICS) increases the background counting rate and degrades the image quality. ICS events correspond to those events in which one or both photons are scattered such that their directions will change and they will be detected in more than one crystal. Parallax is another restricting factor owing to the penetration of the photons into the neighboring crystals. A photon encountering on the detector with an oblique angle with respect to its axis can be first detected not in that detector, but in adjacent ones [1]. More recently, investigators [2, 3, 4] and manufacturers [5] have demonstrated image of noticeably improved quality upon accurate modeling of multiple resolution degrading phenomenon, including ICS and parallax effects [5]. As accurate experimental measurement of ICS and parallax effects is not an easy task and needs dedicated instruments and huge data collection, we have focused on Monte Carlo modeling of these parameters in currently available detection systems in commercial PET scanners. In this study the influence of crystal material on ICS and parallax effect in a specific crystal size has been quantitatively calculated. Alternatively, simulation techniques can be used to perform such measurements, with the added flexibility of easily tracking separate contributions of ICS and parallax effects in degrading the system resolution. As an example, work is currently in progress in our group to individually model the various resolution degrading factors, with the ICS and parallax contributions measured using simulations, as described next, and accurately incorporated in the reconstruction task.

## II. Materials and methods

The MCNP4C Monte Carlo code was used for detailed transport of 511 keV photons originated as pencil beam from a point source toward the central crystal of a block detector consisting of a 13 mm× 13mm crystal array with 4mm × 4mm × 20mm pixel dimension. Monte Carlo N-Particle Transport Code (MCNP) is an advanced MC simulation program, which contains all the necessary cross-section data for neutron, photon, and electron transport calculations [6]. The simulations were performed to investigate the effect of scintillation material on the position detection accuracy (the percentage of events which are correctly positioned in the crystal irradiated) in the detector module as a function of gamma ray incident angle.

Multiple simulations at different gamma ray angles of incidence were performed, in order to investigate the effects of different incidence angles across different crystal materi-

N.A. Abu Osman, F. Ibrahim, W.A.B. Wan Abas, H.S. Abd Rahman, H.N. Ting (Eds.): Biomed 2008, Proceedings 21, pp. 633–636, 2008

als on percent of ICS and parallax events. Furthermore, with altering gamma ray incident angle, the various point source response functions were studied. The evaluation consisted of measuring the full-width-at-half-maximum (FWHM) parameter from the point-source response profiles.

Different types of crystal material including LSO, LYSO, BGO, LuAP and GSO were investigated in this study. A total number of 50000 photons from a point source irradiated the central crystal in each array. Fig. 1 shows the detector module consisting of a 13 mm × 13mm array of 4 mm × 4mm × 20mm crystals. It should be noted that as the main purpose of this study is modeling of ICS and parallax effects only single 511keV photons were used.

Since the goal of this work was assessment of the relations between ICS and crystal material, only the attenuation properties of the crystals were considered.

The code was validated against simulated data published by Shao et al. [7] which studies ICS modeling in animal PET. During the validation process, an 8 × 8 BGO crystal array with 2 × 2 × 10 $mm^3$ size was used exactly similar to the geometry used by Shao et al. The central crystal in blocks was irradiated using a 511keV Pencil beam. In this study, the PDA parameter in BGO block was evaluated with altering the crystal pixel size. Fig. 1 shows a comparison between Shao et al. and MCNP4C data.

A small difference in the results is due to the different cross section libraries used in different Monte Carlo codes. Moreover it should be noted that Shao et al. transport the light as well while we didn't transport the generated light.

All photons fully transported until they were captured in the block or escaped from the geometry. The history of each photon including the coordination, type of interaction, deposited energy and direction cosines for any interaction were registered in a separate matrix. We developed an algorithm

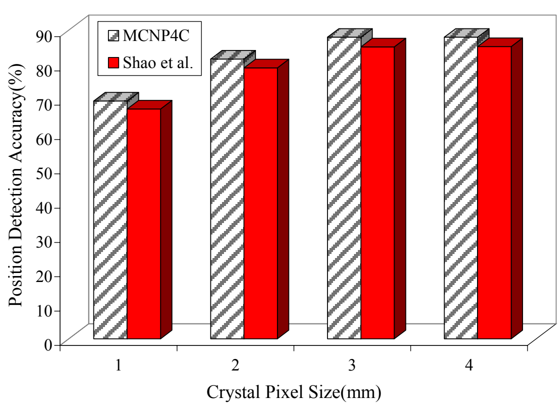


Fig. 1. A comparison between Shao et al. and MCNP4C. A 511keV source with 0° incident angle irradiated a central crystal in an 8×8 array of scintillator.

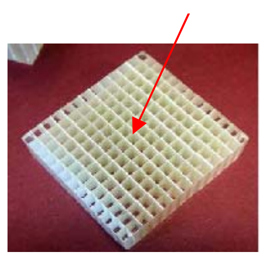


Fig. 2. The 13 × 13 array detector module.

for assessment of the magnitude of ICS and parallax effect in the block detector. In this algorithm, parallax ratio was defined as the number of photons whose first interactions were not in the irradiated crystal to the total number of photons which were detected in the block. The percent of ICS was defined as the ratio of photons for which any of the second or subsequent interactions were in a different crystal than the first interaction crystal to the total number of detected photons in the block. The weighted energy algorithm (extended version of Anger Logic) was used to choose the crystal in which the gamma ray interaction occurred.

### *A. Position detection accuracy and ICS fraction*

In order to assess the effect of crystal material on the position detection accuracy and ICS fraction (compared to all detected events) as a function of gamma ray incident angle, various angles of incidence from 0 to 40 degrees were used for irradiating to the central crystal of module consisting of an 13mm × 13mm array of 4mm × 4mm × 20mm crystals for BGO, LSO, LYSO, GSO and LuAP.

### *B. Parallax*

In order to test the effect of crystal material on parallax, various photons' incidence angle from 10 to 40 degrees were used for irradiating to the central crystal of module consisting of an 13mm × 13mm array of 4mm × 4mm × 20mm crystals for BGO, LSO, LYSO, GSO and LuAP

### *C. Point spread function*

In this method, using a point source located 10 centimeter from the block detector which is shown in the central crystal in the block, the points-spread response FWHM was evaluated (thus in this assessment, the smaller the FWHM, the better the spatial resolution and effective contrast). The amount of deterioration in the spatial resolution was quantified with altering the incident photon angles (0, 30 and 45 degrees), investigated with the aforementioned point source positioning.

## III. Results

Fig. 3 shows the distribution of event centroids (detected positions) calculated by the weighting energy algorithm[7] (extended version of Anger Logic) when irradiating a central crystal within an 13 × 13 array of 4 × 4 × 20 mm$^3$ LSO for irradiation angle of 0 and 45 degree. The parallax effect is clearly seen to occur only at the non-normal angle of incidence, while the ICS events can be seen in both figures.

### *A. Position detection accuracy and ICS*

The effects of crystal material on the position detection accuracy as well as the measured ICS fraction as a function of gamma ray incident angle are shown in Figs. 4(a) and 4(b), respectively. The results show that position detection accuracy and ICS fractions decrease as the gamma ray incident angle is increased. The BGO detector has a higher position detection accuracy and lower ICS than other crystals, as shown in Fig. 4(a) and Fig. 4(b).

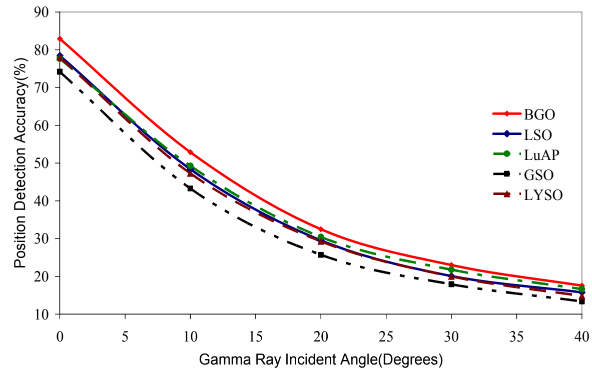


Fig. 4(a) Position detection accuracy for different gamma ray incident angles. A 511 keV source irradiated a central crystal of an 13 × 13 array of 4 mm × 4 mm × 20 mm scintillator.

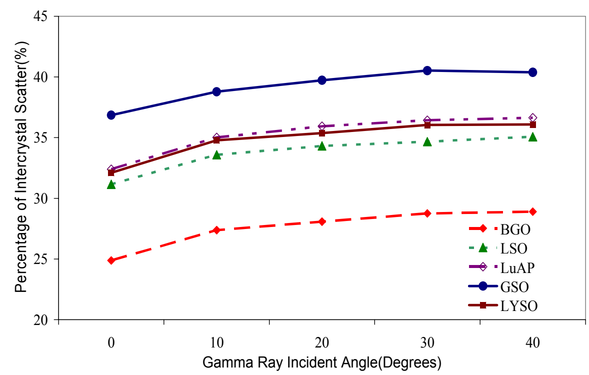


Fig. 4(b) Percentage of intercrystal scatter for different gamma ray incident angles. A 511 keV source irradiated a central crystal of an 13 × 13 array of 4 mm× 4 mm× 20 mm scintillator.

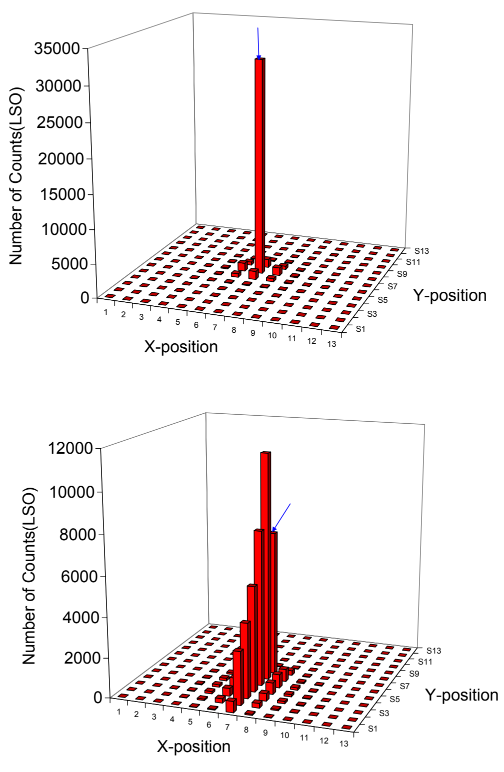


Fig. 3 A scatter plot of the number of photon counts from a 511 keV point source irradiating a central crystal within an 13×13 array of 4×4×20mm$^3$ LSO. The arrow shows the irradiation angle, zero degree (up) and 45 degrees (down).

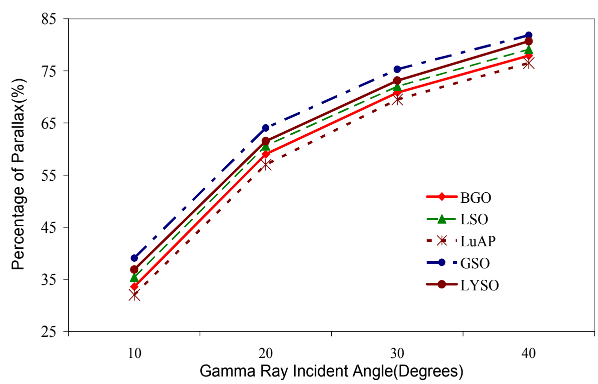


Fig. 5 Percentage of parallax for different gamma ray incident angles. A 511 keV source irradiated a central crystal of an 13 × 13 array of 4 mm× 4 mm× 20 mm scintillator.

Table 1 The amount of FWHM resulting from photon irradiating under 3 angle of 0, 30, 45 degree.

| Scintillator | 0˚ | 30˚ | 45˚ |
|---|---|---|---|
| BGO | 3.54 | 10.45 | 12.12 |
| LSO | 3.66 | 11.11 | 13.33 |
| LuAP | 3.69 | 10.70 | 12.53 |
| GSO | 3.75 | 12.03 | 16.23 |
| LYSO | 3.65 | 11.57 | 14.57 |

### *B. Parallax*

Fig. 5 illustrated the effect of crystal material on parallax as a function of gamma ray incident angle. The LuAP and BGO detectors have lower parallax fractions than other crystals as shown in Fig.5.

### *C. Point spread function*

In Table 1, the measured FWHM value from photon irradiated at 3 angles of 0, 30, 45, for BGO, LSO, LYSO, GSO and LuAP block detectors are shown.

As is revealed from Table 1, under 0, 30, and 45 angles, the measured FWHM values were close for various materials, with BGO and GSO demonstrating the smallest and largest relative FWHM values, respectively; i.e. among the selected crystals, BGO exhibited a slightly higher spatial resolution.

## IV. Discussion

The increase in ICS is due to forward angle scattering towards neighboring crystals in direction of incident oblique 511 keV photons. The results show that by increasing incidence angle the percentage of parallax events were considerably increased. The greatest amount of the parallax and ICS events belonged to the GSO crystal and the smallest amount of them belonged to the BGO crystal. Although the BGO crystals shows better performance regarding to the analysis of ICS and parallax effect, the higher light output and lower decay time of LSO and LYSO continue to make them as the crystals of choice for manufacturers.

## V. Conclusion

This study used the MCNP4C general-purpose Monte Carlo code for accurate modeling of ICS and parallax effects in different crystals. The present context consisted of investigating the aforementioned effects at 511 keV photon irradiation, as is relevant for PET studies. Although the transport of 511 keV photons using the Monte Carlo method is time consuming, the data provide detailed information about photons' interaction within the crystal. This information can be very useful for accurate measurement and modeling of ICS and parallax effects (as function of crystal material and crystal dimension) into reconstruction algorithms to yield higher-resolution images, which is currently being actively investigated by our group. The results indicate that the MCNP4C general purpose Monte Carlo code with some small adjustment in the appropriate MCNP cards is a useful tool for investigation of photons interaction in PET block detectors in order to accurately model the ICS and parallax behavior for the purpose of resolution recovery in state-of-the-art PET image reconstruction algorithms.

## References


1. Bream A., Llatas M. C., Chesi E., Correia j. G., Garibaldi F., Joram C., et al. (2004) Feasibility of a novel design of high resolution parallax-free Compton enhanced PET scanner dedicated to brain research. Phys. Med. Biol. 49:2547-2562.
2. Qi J., Leahy R. M., Chinghan H., Farquhar T. H., and Cherry S. R. (1998) Fully 3D Bayesian image reconstruction for the ECAT EXACT HR+.IEEE Trans. Nucl. Sci. 45:1096-1103.
3. Selivanov V. V., Picard Y., Cadorette J., et al. (2000) detector response models for statistical iterative image reconstruction in high resolution PET. IEEE Trans. Nucl. Sci.47:1168-1175. .
4. Reader A. J.,Julyan P. J.,Williams H., et al. (2003) EM Algorithm System Modeling by Image-Space Techniques for PET reconstruction IEEE Trans. Nucl. Sci., 50: 1392-1397.
5. Casey M. E. ( 2007) Point spread function reconstruction in PET. Siemens Medical Solution, Knoxville, USA.
6. Rodenas J., Martinavarro A, Rius V. (2000) Validation of the MCNP code for the simulation of Ge-detector calibration. Nucl. Instrum. Meth. Phys. Res. 450:88-97.
7. Shao Y., Cherry S. R., Siegel S., and Silverman RW (1996) A study of Inter-Crystal Scatter in Small Scintillator Arrays Designed for High Resolution PET Imaging. IEEE Trans. Nucl. Sci. 43:1938-1944.



Corresponding Author:
Author: Saeed Sarkar
Institute: School of Medicine, Medical Sciences/ Tehran University
Street: Pour Sina
City: Tehran
Country: Iran
Email: sarkar@sina.tums.ac.ir